Combined manual and automated immunophenotypisation identified disease-specific peripheral blood immune subpopulations in rheumatoid arthritis, ankylosing spondylitis and psoriatic arthritis

Šućur, Alan; Jajić, Zrinka; Ikić Matijašević, Marina; Stipić Marković, Asja; Flegar, Darja; Lukač, Nina; Kelava, Tomislav; Kovačić, Nataša; Grčević, Danka

Repository / Repozitorij:

Dr Med - University of Zagreb School of Medicine Digital Repository

Combined manual and automated immunophenotypisation identified disease-specific peripheral blood immune subpopulations in rheumatoid arthritis, ankylosing spondylitis and psoriatic arthritis

Dr. Alan Šućur[1], Prof. Zrinka Jajić[2], Dr. Marina Ikić Matijašević[3], Prof. Asja Stipić Marković[3], Dr. Darja Flegar[1], Dr. Nina Lukač[1], Prof. Tomislav Kelava[1], Prof. Nataša Kovačić[1], Prof. Danka Grčević[1]

[1] Croatian Institute for Brain Research, Laboratory for molecular immunology, University of Zagreb School of Medicine, Salata 12, Zagreb-HR 10000, Croatia

[2] Clinical Hospital Center "Sestre Milosrdnice", Department of Rheumatology, Physical Medicine and Rehabilitation, University of Zagreb School of Medicine, Vinogradska cesta 29, Zagreb-HR 10000, Croatia

[3] Clinical Hospital "Sveti Duh", Department of Clinical immunology and pulmology, Sveti Duh 64, Zagreb-HR 10000, Croatia

Corresponding author and author to contact for reprints: Prof. Danka Grčević, address: Department of Physiology and Immunology, University of Zagreb Medical School, Šalata 3, 10000 Zagreb, Croatia, telephone: +385 1 4566 944, e-mail: danka.grcevic@mef.hr

Short title: Immunophenotypisation in inflammatory arthritis

Abstract

Objective: Rheumatoid arthritis (RA), ankylosing spondylitis (AS) and psoriatic arthritis (PsA) are associated with abnormal immune cell functions. We combined manual and automated profiling in subpopulations of T-cells, B-cells and monocytes; in parallel to functional testing and clinical correlation. **Methods:** Using flow cytometry, we analyzed expression of CCR4, CCR6 and CXCR5 on helper and cyotoxic T-cells, CD32B and C86 on naïve and memory B-cells, and CCR1, CCR2, CCR4 and CXCR4 on monocytes in chronic high-disease activity patients to identify peripheral blood subpopulations. Cell activation, proliferative capability and osteoclastogenic effects were tested in vitro. Comparison with synovial compartment, clinical data and anti-TNF treatment were added to peripheral blood analysis. **Results:** PsA had lower double-negative T-cell frequency, while RA had lower double-positive T-cell frequency and expanded Th1-like population. CD32B expression was increased on naïve and memory B-cells in AS and associated with disease activity. CCR6$^+$ and CXCR5$^+$ cytotoxic T-cells and CD32B$^+$ naïve and memory B-cells were highly enriched within synovial compartment. T-cells and B-cells from AS exhibited enhanced activation and proliferation in vitro, whereas T-cell conditioned medium from RA produced increased osteoclastogenic effect. CCR1 and CXCR4 were upregulated on osteoclastogenic monocyte subset of RA, AS and PsA patients. Bioinformatic Citrus analysis identified additional T-cell, B-cell and monocyte clusters specifically associated with each disease. **Conclusion:** By combining manual and automated data analysis, our study revealed several disease-specific immune cell subpopulations, particularly cytotoxic T-cell subsets in RA and memory B-cell subsets in AS, which may serve as an indicator of active disease or possible therapeutic target.

Keywords: lymphocyte, monocyte, rheumatoid arthritis, ankylosing spondylitis, psoriatic arthritis

Introduction

In rheumatic diseases, aberrancies in inflammatory and immune cell populations, precipitated by genetic and environmental factors, promote autoimmunity and persistent inflammation, resulting in both systemic and local pathology (1-3). Chronic systemic immune inflammation represents a central hallmark of rheumatic diseases and accounts for substantially increased cardiovascular risk and associated comorbidities in these patients. On the local level, inflammation and associated cytokine milieu alters bone cell activity, resulting in bone and joint pathology (4, 5).

While there has been substantial improvement in clinical outcomes of inflammatory joint diseases since the introduction of novel therapeutical approaches, the crucial component(s) responsible for the pathogenesis of these diseases have yet to be elucidated and, consequently, current treatment remains more or less non-specific. Moreover, some patients exhibits poorly controlled disease, having high disease activity and progression despite prolonged treatment (6). Rheumatoid arthritis (RA), psoriatic arthritis (PsA) and ankylosing spondylitis (AS) are the most common inflammatory rheumatic diseases (7). They differ substantially in immune mechanisms as well as in the patterns of bone and cartilage damage (8). RA commonly manifests as a symmetric and erosive arthritis typically affecting small and medium-sized joints, with erosion resulting from a continuous inflammatory attack of the synovial membrane on bone (1). In RA, T-cells, B-cells, and the concerted interaction of pro-inflammatory cytokines play key roles in disease pathophysiology. T-cells detected in established disease have features of both Th1 and Th17, with most T-cells specific for citrullinated tetramers being of Th1 phenotype. RA mostly presents as a seropositive arthritis due to autoantibody production, such as rheumatoid factor (RF) and anti-citrullinated protein antibodies (aCPA),

which are closely related to the chronicity of the disease (9, 10). PsA is a more heterogeneous inflammatory disease, varying from mild monoarthritis to severe polyarthritis, and may also involve the axial skeleton and the entheses (2). Chronic inflammation mediated by activated T-cells and macrophages is thought to play important roles in the induction of articular inflammation and destruction (11). AS is a systemic inflammatory disorder that primarily affects the sacroiliac joints and the spine, but can also affect peripheral joints and entheses (3). Although the disease-associated HLA-B27 would be predicted to generate autoreactive CD8 T-cells, T-cell targeting therapies have shown unpromising results. Moreover, effectiveness of rituximab suggests the role of B-cells and immune complexes (12).

Despite significant clinical improvements being achieved in the outcome of inflammatory rheumatic diseases, systemic disturbances in immune cell populations seem to persist in chronically active forms, with these cells permanently homing to affected joints and triggering pathology (8). The primary aim of our study was to associate specific aberrancies of circulatory lymphocyte and monocyte subsets with a distinct form of rheumatic disease, by evaluating manual and bioinformatic phenotypisation extended by functional characterization and correlations with clinical parameters. Since peripheral blood samples are readily obtainable as a part of routine assessment, it would be beneficial to elucidate one or more key disease specific immune cell populations, which may indicate highly active disease and serve as possible therapeutic target. As secondary objectives, we set out to evaluate, firstly, whether these specific aberrancies carry over into the synovial compartment and, secondly, if their frequency changes in response to anti-TNF therapy.

Materials and methods

Patients

Arthritic patients (RA, n=30; AS, n=22; and PsA, n=22), admitted to the Department of Rheumatology, Physical Medicine and Rehabilitation at Clinical Hospital Center "Sestre Milosrdnice" or to the Department for Clinical Immunology, Rheumatology and Pulmology at Clinical Hospital "Sveti Duh", were included in the study after obtaining approval from the Ethics Committee and informed consent from patients (Table 1). A rheumatology specialist established the diagnosis of RA based on the American College of Rheumatology (ACR) 2010 criteria, AS based on 1984 Modified New York classification criteria, while PsA according to the Moll and Wright criteria (13-15). Patients were enrolled based on: age of 40 or more years; disease duration of at least 5 years after diagnosis was established by a specialist; being on therapy consisting of non-steroid anti-inflammatory drugs (NSAID), disease-modifying anti-rheumatic drugs (DMARD) and/or glucocorticoids (with no history of biological therapy); and having Disease activity score including a 28-joint count (DAS28)>3.2 for RA patients, Ankylosing spondylitis disease activity score (ASDAS)>2.1 for AS patients, or Disease activity index for psoriatic arthritis (DAPSA)>14 for PsA patients (16-18). In patients with significant accumulation of synovial fluid in the knee (n=8 RA, n=3 PsA), the effusion was aspirated and analyzed for immune cell subpopulations as later described. Control subjects (CTRL, n=24), aged 40 years or above,were admitted to same institutions due to non-inflammatory etiology, with no previous history of arthritic or autoimmune diseases. An additional, smaller, group of patients (RA n=3, AS=5, PsA=8) of similar age and disease duration scheduled for anti-TNF treatment (etanercept 50 mg weekly or adalimumab 40 mg every two weeks) was followed up by analyzing their samples before, 1 month and 3 months after introduction of anti-TNF therapy (19, 20).

Isolation of mononuclear cells

Peripheral blood mononuclear cells (PBMCs) were separated by centrifugation (20 min at 600 g) with Histopaque (Sigma-Aldrich, Saint Louis, MO, USA) and subjected for flow cytometry phenotyping, lymphocytic proliferation assay and osteoclastogenic cocultures. Synovial fluid-derived cells were isolated by sequential centrifugation (5 min at 100 g) of aspirated effusion diluted in increasing amounts of phosphate-buffered saline and phenoytped using flow cytometry. Cell viability, checked by Trypan Blue exclusion, was determined to always be greater than 95%.

Flow cytometry

Phenotype characterization of PBMCs was performed on the Attune flow cytometer (Life Technologies, ABI, Carlsbad, CA, USA) and analyzed by FlowJo software (TreeStar, Ashland, OR, USA FlowJo LLC, Ashland, OR USA). Cells were labelled using commercially available monoclonal antibodies (eBiosciences;San Diego, CA, USA). Flow cytometry gating was performed according to suggested strategies (8, 21-23) for T-cell helper (22, 23), T-cell cytotoxic, B-cell (21) (with additional analysis of CD32B and CD86 expression (24, 25)) and osteoclast progenitor-enriched monocyte (with additional analysis of CCR1, CCR2, CCR4 and CXCR4) subpopulations (26) (phenotype noted in Table 2, gating strategy in Supplementary figure 1, antibody-producing clones noted in Supplementary table 1).

Lymphocyte proliferation and activation assay

PBMCs of CTRL, RA, AS and PsA samples were first labeled with Cell Proliferation Dye eFluor 670 (eBiosciences), according to the manufacturer instruction, then with anti-CD3 for T-cells and anti-CD19 for B-cells, and sorted using BD FACSAria II (BD Biosciences, Franklin Lakes, NJ, USA). The mitogenic pulse was carried out by adding 50 ng/mL Phorbol 12-myristate 13-acetate (PMA) and 0.5 ng/mL calcium ionophore A23187 (both from Sigma-Aldrich) and incubating for 3 hours at 37 °C. The cells were washed and plated into 96-well plates at a density of 250,000 T-cells per well and 70,000 B-cells per well in RPMI with 10% fetal bovine serum (FBS) and cultured for 72h. Corresponding non-pulsed lymphocytes were used as non-stimulated controls. Upon harvesting, lymphocytes were labeled with anti-CD69 as a marker of activation (27) and analyzed on Attune flow cytometer, while proliferation was evaluated as the percent of divided cells by assessing Proliferation Dye eFluor 670 fluorescence intensity and using the FlowJo Proliferation platform (setting the number of peaks to 2).

Osteoclastogenic culture treated by lymphocyte-conditioned medium

Osteoclast progenitor-enriched monocytes (CD3$^-$CD19$^-$CD56$^-$CD11b$^+$CD14$^+$) were sorted from peripheral blood and plated at a density of $4{\times}10^4$ cells per well in 96-well plate in α-MEM/10% FBS, supplemented with osteoclastogenic growth factors, 30 ng/mL of recombinant human (rh) macrophage colony-stimulating factor (M-CSF) and 100 ng/mL rh receptor activator of nuclear factor-kappaB ligand (RANKL) (R&D Systems, NE Minneapolis, MN, USA) and adittionaly treated with lymphocyte-conditioned medium in the dillution 1:3. At day 11–13 of culture, cells were stained for tartrate-resistant acid phosphatase (TRAP) using a commercially available set of chemicals according to the manufacturer's instructions (Leukocyte acid phosphatase kit; Sigma-Aldrich Corp.). Using light microscopy on Axiovert

200 (Carl Zeiss, AG, Oberkochen, Germany), osteoclasts were identified as TRAP$^+$ cells with two or more nuclei per cell.

Bioinformatic analysis

Flow cytometry data was analyzed in an automated hierarchical clustering algorithm and analysis software Citrus v0.8 22 using R v3.5.2, as described by Bruggner et al. (28), which organizes cells into clusters depending on the expression of various markers. The autogating hierarchy of nodes is then depicted in cluster plots, with node size being relative to the number of cells, and color marking the expression level of a noted marker, followed by group comparison for defined populations. Analyses were performed by using data from all groups to build a tree in Citrus for each staining panel, with randomized sampling of 5000 events, transformed with a cofactor of 150, from individual sample and defining smallest cluster or subpopulation size as 5% of cells in total data. Analysis between groups was done on account of cell abundance in a cluster using "significance analysis of microarrays" (sam) model which identified values associated with a particular group. For T-cell panel, CD3$^+$ cells were exported from FlowJo with applied compensation and then clustered and analyzed in Citrus on the basis of expression of CD4, CD8, CCR4, CCR6, CXCR5. For B-cell panel, CD19$^+$ cells were exported from FlowJo and then analyzed on account of IgD, CD27, CD38, CD86, CD32B. For monocytes, CD3$^-$CD19$^-$CD56$^-$CD11b$^+$ cells were exported and then analyzed on account of CD14, CD115 and either CCR2 and CCR4 or CCR1 and CXCR4.

Statistical analysis

Data were presented as median±interquartile range (IQR) for continuous variables or categorized for categorical variables. Statistical analysis was performed using non-parametric Kruskal-Wallis test; disease-to-control differences were tested by Mann-Whitney test. Correlations were done using rank correlation and Spearman's coefficient rho (ρ) with its 95% confidence interval (CI). Statistical analyses were performed using MedCalc for Windows, version 9.4.2.0 (MedCalc Software, Ostend, Belgium). For all experiments, α-level was set at 0.05.

Results

Decreased double-negative T-cells in psoriatic arthritis and double positive T-cells in rheumatoid arthritis

General T-cell populations (total $CD3^+$, helper $CD3^+CD4^+$, cytotoxic $CD3^+CD8^+$) did not differ in frequency across the groups (Supplementary figure 1D, Figure 1A). However, double-positive ($CD4^+CD8^+$) T-cells, were of lower frequency in RA. On the other hand, PsA had lower frequency of circulating double-negative ($CD4^-CD8^-$) T-cells (Figure 1A). In our study, this population was enriched among synovial-fluid derived cells in RA patients (Supplementary table 2). In adittion, we followed-up a small group of arthritic patients under anti-TNF therapy and observed a tendency of recovery in initially decreased circulatory double-positive and double-negative T-cells by anti-TNF, that was statistically significant for double-negative T-cells in PsA paired samples (Supplementary figure 2).

Of helper T-cell subpopulations, only Th1-like (CD4$^+$CCR4$^-$CCR6$^-$) cells had significantly increased frequency in RA (Figure 1B). Furthermore, the Th1-like cells strongly positively correlated with Clinical Disease Activity Index (CDAI) (rho=0.821, p=0.021; Figure 2).

Cytotoxic (CD3$^+$CD8$^+$) T-cell subpopulations were altered in RA (Figure 1C), with a specific increase in CCR6$^+$ (early effector memory) and CXCR5$^+$ (follicular) cytotoxic lymphocytes. Cytotoxic lymphocytes expressing CCR6 were also significantly increased in synovial fluid of RA patients (Supplementary table 2) and strongly positively correlated with the number of tender joints (rho=0.811, p=0.027; Figure 2), suggesting possible intra-articular accumulation.

Increased CD32B$^+$ B-cell subpopulations in ankylosing spondylitis associated with disease activity indices

Total B-cells (CD19$^+$) were significantly increased in our group of patients with long disease duration and high disease activity, specifically in RA and, more pronounced, in AS (Supplementary figure 1D). Other than a slight increase in frequency of naïve B-cells (IgD$^+$CD27$^-$) in PsA, there were no significant changes among main B-cell subpopulations across groups (Figure 3A). Thus, we proceded to analyze expression of inhibitory receptor CD32B (antibody Fc-receptor II B, FcγRIIB) and costimulatory molecule CD86 (B7-2), both of which have been implied in development of autoimmune diseases, including inflammatory arthritis (29, 30).

There was a notable increase in CD32B expression on naïve (IgD$^+$CD27$^-$) and memory (unswitched IgD$^+$CD27$^+$, class-switched IgD$^-$CD27$^+$ and double-negative IgD$^-$CD27$^-$) B-cells in AS, on plasmablasts (IgD$^-$CD27$^+$CD38$^+$) in RA and class-switched memory B-cells in PsA

(Figure 3B). Furthermore, CD32B expression on double-negative memory B-cells was strongly positively associated with both Bath ankylosing spondylitis disease activity index (rho=0.721, p=0.019) and, especially, ankylosing spondylitis disease activity score (rho=0.794, p=0.006; Figure 2). In addition, CD32B^{+} subsets of both naïve and memory B-cells accumulated in RA and PsA synovial fluid (Supplementary table 3). In contrast to CD32B, changes in CD86 expression were unremarkable, with only significant finding of reduced CD86^{+} class-switched memory B-cell subset in AS (4.8% [3.9-6.1] in AS vs 7.0% [5.1-8.5] in CTRL, p<0.001).

Bioinformatics analysis links T-cell clusters with rheumatoid arthritis and B-cell clusters with ankylosing spondylitis

Using Citrus algorithm to automatically cluster cells in specific nodes depending on surface marker expression and unbiasely assess the generated hierarchical trees of each panel, several specific cell subpopulations were detected for each disease.

In the T-cell panel, Citrus detected two clusters of cells which had significantly altered frequency in RA (Figure 4). First cluster (279966) which contained a subpopulation of helper T-cells (CD4^{+}CD8^{-}), positive for both CCR6 and CXCR5, but negative for CCR4, was virtually absent in RA samples; second cluster (279969) consisted of double-positive (CD4^{+}CD8^{+}) T-cells positive for both CCR4 and CCR6, but negative for CXCR5, was of increased frequency in RA.

Citrus analysis of the B-cell panel revealed two distinct subpopulations associated with AS (Figure 5). One cluster (249947) had a decreased subpopulation of naïve B-cells (IgD^{+}CD27^{-}) which was positive for CD38, while the other cluster (249941) had an increased subpopulation of unswitched memory B-cells (IgD^{+}CD27^{+}) positive for both CD32B and CD38, but negative for CD86.

Enhanced activation and proliferation of both T- and B-cells from ankylosing spondylitis

In addition to phenotype, we assessed the activation and proliferation potential of peripheral T- and B-cells in a small group of RA, AS and PsA samples. Sorted T- and B-cells were treated by mitogenic pulse and assessed for the activation and proliferation profile compared to corresponding unstimulated cells.

Both T- and B-cells were found to significantly upregulate CD69, as a marker of activation, and contained more divided cells in AS samples (Figure 6). There was a similar tendency in PsA samples, though it was only significant for the number of divided T-cells, whereas there were no significant differences between RA samples and controls.

Increased CCR1$^+$ and CXCR4$^+$ osteoclastogenic monocyte subsets in rheumatoid arthritis, ankylosing spondylitis and psoriatic arthritis

Based on our previous work, we selected a double-positive, CD11b$^+$CD14$^+$, monocytic subpopulation expressing CD115, noted to contain peripheral osteoclast progenitors, and profiled it for chemokine receptors - CCR1, CCR2, CCR4 and CXCR4 (26). Even though the general subpopulation did not differ in frequency across the groups, its expression of CCR1 and CXCR4 was significantly increased in RA, AS and PsA (Figure 7).

Since double-positive monocytes exhibit osteoclastogenic potential and can contribute to joint and bone destruction in inflammatory arthritis (26), we also performed a functional osteoclastogenic assay by co-culture of a sorted subset of peripheral monocytes and T-cell-conditioned medium, which is known to contain osteoclastogenic factors (8) (Supplementary

figure 3). Supernatant obtained from unstimulated lymphocytes did not alter the osteoclastogenic potential of sorted progenitors. However, supernatant from mitogenically-pulsed control T-cells significantly enhanced osteoclastogenesis and the effect was further stimulated by supernatants from mitogenically-pulsed RA T-cells, indicating a change in their secretory profile, even though the activation and proliferation profile was similar to that of control.

Bioinformatics analysis reveals monocyte clusters associated with psoriatic arthritis, ankylosing spondylitis and rheumatoid arthritis

Monocytes were analyzed by two panels using Citrus algorithm. The first panel (Figure 8A) detected a cluster (261174) of monocytes (CD11b$^+$CD14$^+$) expressing CD115 and double positive for CCR1 and CXCR4 which was of significantly higher frequency in PsA and AS samples (Figure 8A). Two detected clusters in the second panel were indifferent in regards to CD115 expression (Figure 8B). The first cluster (296636) contained a monocyte subpopulation of CD11b$^+$CD14$^+$ cells that express CCR2 and was of increased frequency in RA, AS and PsA. The second cluster (296627) contained CD11b$^+$CD14$^-$ cells positive for CCR4 and negative for CCR2, and was of lower frequency in RA and AS.

Discussion

Phenotyping of peripheral immune cell populations has been widely appreciated as the method to assess autoimmune diseases. However, by following predefined gating strategies based on the preceding research, it is not possible to fully utilize the advances in flow cytometry

interpretation and to profile novel disease-specific cell subsets. Moreover, rapid technical improvements of cytometry platforms, while increasing the effectiveness and reducing time for acquiring, have been generating high-dimensional datasets inappropriate for meaningful and uniformed analysis using standard bivariate dot-plots (26, 31, 32). To overcome these limitations, automated cytometry analysis was introduced to enable comprehensive and unbiased approach in fraction of time and labor. Among new algorithms and software, Citrus is, so far, the only one enabling completely automated identification of unique cell subpopulations associated with a particular disease in an objective and reproducible way. However, the proposed algorithms still need to be applied in different settings and experimentally verified to become widely accepted as method for flow cytometry data interpretation (28, 33). By combining data of manual/automated immunophenotyping, functional analysis and clinical assessment, we identified several pathognomonic immune cell subpopulations in different forms of arthritis (Figure 9).

RA patients mostly presented with a disturbed peripheral T-cell compartment, including increased proportion of Th1-like ($CD4^+CCR4^-CCR6^+$) cells. RA is traditionally considered as a Th1-predominant disease with the expansion of citrulline-specific autoreactive Th1 cells that contribute to aCPA production (34). In addition, Citrus identified a cluster of Th9-like cells ($CD4^+CCR6^+CCR4^-$) expressing the marker of Tfh, CXCR5, as absent from peripheral blood of RA patients. Th9 cells accumulate in RA synovium, whereas CXCR5 serves to attract T-cells to germinal centers, thus this subpopulation might stimulate B-cell differentiation inside the synovial germinal center-like structures (35). Moreover, expansion of peripheral $CD8^+CCR6^+$ early effector memory cytotoxic T-cells was found in RA, which accumulated in synovial fluid and associated with number of tender joints. Recent human studies indicate that CD8 T-cell may be important for establishment of germinal center-like structures in the inflamed synovium, secreting cytokines that positively correlate with disease activity (36, 37).

In particular, early effector memory cells mainly secrete proinflammatory Th1 cytokines, whereas immature effector memory T-cells are predominantly of secretory Th2 nature and are associated with immune-mediated skin diseases (38). We also observed a significant decrease of double-negative ($CD4^-CD8^-$) T-cells in PsA and double-positive ($CD4^+CD8^+$) T-cells in RA, subsets associated with autoimmune, malignant and graft-versus-host diseases (39, 40). Interestingly, Citrus revealed enlarged $CCR4^+CCR6^+$ subset among double-positive T-cells in RA that has not been previously studied. Double-negative T-cells have been detected inside entheses of AS and skin lesions of PsA patients (41, 42), whereas we found this population expanded within synovial compartment in RA and recovered among PBMCs upon anti-TNF therapy in PsA patients. However, the roles of double-positive and double-negative populations remain largely unclear since studies are giving controversial results (43, 44).

The most striking findings within B-cell compartment were, unexpectedly, found in AS. AS is considered as a seronegative spondylarthritides with dominantly abberant autoreactive T-cells and dendritic cells, whereas RA is referred to as a prototype of a seropositive arthritis and B-cell pathology, emphasized by effectiveness of rituximab (45). However, in recent years, it has been shown that AS develops even in total absence of $CD8^+$ T-cells, with several types of newly discovered autoantibodies (including anti-CD47, anti-sclerostin and anti-noggin), thereby shifting focus to B-cell importance (12). Namely, we found increased CD32B expression on naïve and memory B-cell subpopulations in AS, particularly on double-negative (IgD^-CD27^-) memory B-cells that correlated positively with disease activity. Still controversial, double-negative B-cells have been proposed to be exhausted or anergic B-cells, a product of abnormal germinal center reaction, or to be a unique population formed extra-folliculary. This subset has been upregulated in some autoimmune or malignant diseases and, moreover, the expression of CD32B on double-negative B-cells was found to correlate with disease activity in systemic sclerosis (21, 46). Citrus also detected more abundant unswitched memory B-cells with high

expression of inhibitory CD32B and virtually absent co-stimulatory CD86 in AS. Unswitched memory B-cells seem to have regulatory characteristics, linked with improved clinical outcomes in inflammatory states (47). Moreover, CD32B$^+$ subsets of naïve and memory B-cells were highly enriched in the synovial compartment of both RA and PsA patients. We also found that plasmablasts in RA increasingly expressed CD32B, shown to be associated with low level of autoantibodies (48, 49). Since CD32B (FcγRIIb) acts as an inhibitory receptor important for peripheral tolerance (50), enhanced expression could represent a compensatory reaction to abnormal activation of B-cells. Citrus also revealed a decrease in CD38$^+$ naïve B-cells, that we have not detected manually (since CD38 is used as a plasmablast marker on memory B-cells). However, CD38 deficiency has been noted to lead to autoimmunity (51), while overexpression stimulates regulatory B-cell function (52). In the functional assay, activation marker CD69 was upregulated upon in vitro polyclonal B- and T-cell activation in AS, in parallel to enhanced lymphocyte proliferative response. While the T-cell response in AS confirms tradionally mentioned T-cell aberrancies, the enhanced B-cell activation and proliferation reinforces the notion of B-cell abnormalities in AS.

Changes in peripheral osteoclast progenitor-enriched monocytes were more uniform between arthritis subtypes, showing increased CCR1 and, especially, CXCR4 expression. We have previously shown that CXCR4 expression on peripheral monocytes positively correlates with resorptive and immune parameters in RA, whereas anti-TNF therapy has decreased CXCR4 expression (26). CXCR4 has been shown to play an important role in development of psoriasis, while CXCR4 inhibition suppressed osteogenic potential in AS (53-55). CCR1 has been mostly studied in the context of RA, considering its role in monocyte attraction into the affected joints (56). Furthermore, a cluster of monocytes co-expressing CCR1 and CXCR4 was identified by Citrus to be pathognomonic for AS and PsA. In addition, Citrus singled out a subset of CCR2$^+$ monocytes which was enlarged in all three forms of arthritis, while a subset of CCR4$^+$

monocytes was decreased in RA and AS. We have previously shown that ligands for CCR2 and CCR4 enhanced differentiation of osteoclast progenitors defined within $CD11b^+CD14^+CD115^+$ subset of peripheral monocytes in RA (26, 57). In an in vitro functional assay, we observed enhanced osteoclastogenic effect of conditioned medium from mitogen-stimulated RA T-cells, indicating they may produce osteoresorptive mediators in a stimulatory environment.

While the study maintains the possibility to distinguish abberances across different diseases, the approach did have limitations in the ability to test secondary objectives. Thus, supplementary data pertaining to anti-TNF effect and synovial fluid anaylsis are primarily indicative due to small sample sizes. Furthermore, inclusion criteria and clinical characteristics of enrolled patients did not allow analysis of possible differences according to disease activity subgroups (in particular remitting/low activity patients). Finally, PsA patients were diagnosed according to the Moll and Wright criteria, instead of widely accepted CASPAR criteria, but for chronic high activity disease both should have similar sensitivity and thus, we believe, should not have had a notable impact on our results. Despite the listed limitations, we believe that the study succesfuly elucidated changes related to rheumatic diseases and evaluated its disease-specificity.

To conclude, our results revealed significant aberrancies in peripheral lymphocyte and monocyte populations, in particular phenotypic and functional abnormalities in, traditionally overlooked, B-cells in AS (Figure 9). Both manual gating strategies and automated software emphasized the importance of enriched $CD32B^+$ subsets that are further expanded within synovial compartment. Several populations, not fully defined in existing literature, emerged as possible additional targets, including early effector memory cytotoxic T-cell subsets in RA, which could accumulate in the affected joints. Identified subpopulations may serve as disease specific markers that could further be used as indicators of therapeutic response or as novel therapeutic targets.

Acknowledgements

References

1.   Malmstrom V, Catrina AI, Klareskog L. The immunopathogenesis of seropositive rheumatoid arthritis: from triggering to targeting. Nat Rev Immunol. 2017;17(1):60-75.

2.   Barnas JL, Ritchlin CT. Etiology and Pathogenesis of Psoriatic Arthritis. Rheum Dis Clin North Am. 2015;41(4):643-63.

3.   Ranganathan V, Gracey E, Brown MA, Inman RD, Haroon N. Pathogenesis of ankylosing spondylitis - recent advances and future directions. Nat Rev Rheumatol. 2017;13(6):359-67.

4.   Rhoads JP, Major AS, Rathmell JC. Fine tuning of immunometabolism for the treatment of rheumatic diseases. Nat Rev Rheumatol. 2017;13(5):313-20.

5.   Benatti FB, Pedersen BK. Exercise as an anti-inflammatory therapy for rheumatic diseases-myokine regulation. Nat Rev Rheumatol. 2015;11(2):86-97.

6.   Schett G, Coates LC, Ash ZR, Finzel S, Conaghan PG. Structural damage in rheumatoid arthritis, psoriatic arthritis, and ankylosing spondylitis: traditional views, novel insights gained from TNF blockade, and concepts for the future. Arthritis Res Ther. 2011;13 Suppl 1:S4.

7.   Michelsen B, Fiane R, Diamantopoulos AP, Soldal DM, Hansen IJ, Sokka T, et al. A comparison of disease burden in rheumatoid arthritis, psoriatic arthritis and axial spondyloarthritis. PLoS One. 2015;10(4):e0123582.

8.   Sucur A, Katavic V, Kelava T, Jajic Z, Kovacic N, Grcevic D. Induction of osteoclast progenitors in inflammatory conditions: key to bone destruction in arthritis. Int Orthop. 2014;38(9):1893-903.

9.   Yap HY, Tee SZ, Wong MM, Chow SK, Peh SC, Teow SY. Pathogenic Role of Immune Cells in Rheumatoid Arthritis: Implications in Clinical Treatment and Biomarker Development. Cells. 2018;7(10).

10.   Calabresi E, Petrelli F, Bonifacio AF, Puxeddu I, Alunno A. One year in review 2018: pathogenesis of rheumatoid arthritis. Clin Exp Rheumatol. 2018;36(2):175-84.

11.   Diani M, Altomare G, Reali E. T cell responses in psoriasis and psoriatic arthritis. Autoimmun Rev. 2015;14(4):286-92.

12.   Smith JA. Update on ankylosing spondylitis: current concepts in pathogenesis. Curr Allergy Asthma Rep. 2015;15(1):489.

13.   Aletaha D, Neogi T, Silman AJ, Funovits J, Felson DT, Bingham CO, 3rd, et al. 2010 Rheumatoid arthritis classification criteria: an American College of Rheumatology/European League Against Rheumatism collaborative initiative. Arthritis Rheum. 2010;62(9):2569-81.

14.   Moll JM, Wright V. Psoriatic arthritis. Semin Arthritis Rheum. 1973;3(1):55-78.

15.   van der Linden S, Valkenburg HA, Cats A. Evaluation of diagnostic criteria for ankylosing spondylitis. A proposal for modification of the New York criteria. Arthritis Rheum. 1984;27(4):361-8.

16.   Inoue E, Yamanaka H, Hara M, Tomatsu T, Kamatani N. Comparison of Disease Activity Score (DAS)28- erythrocyte sedimentation rate and DAS28- C-reactive protein threshold values. Ann Rheum Dis. 2007;66(3):407-9.

17.   Machado P, Landewe R, Lie E, Kvien TK, Braun J, Baker D, et al. Ankylosing Spondylitis Disease Activity Score (ASDAS): defining cut-off values for disease activity states and improvement scores. Ann Rheum Dis. 2011;70(1):47-53.

18.   Schoels MM, Aletaha D, Alasti F, Smolen JS. Disease activity in psoriatic arthritis (PsA): defining remission and treatment success using the DAPSA score. Ann Rheum Dis. 2016;75(5):811-8.

19.   Gossec L, Smolen JS, Ramiro S, de Wit M, Cutolo M, Dougados M, et al. European League Against Rheumatism (EULAR) recommendations for the management of psoriatic arthritis with pharmacological therapies: 2015 update. Ann Rheum Dis. 2016;75(3):499-510.

20.   Smolen JS, Landewe R, Bijlsma J, Burmester G, Chatzidionysiou K, Dougados M, et al. EULAR recommendations for the management of rheumatoid arthritis with synthetic and biological disease-modifying antirheumatic drugs: 2016 update. Ann Rheum Dis. 2017;76(6):960-77.

21.   Centuori SM, Gomes CJ, Kim SS, Putnam CW, Larsen BT, Garland LL, et al. Double-negative (CD27(-)IgD(-)) B cells are expanded in NSCLC and inversely correlate with affinity-matured B cell populations. J Transl Med. 2018;16(1):30.

22.   Luckheeram RV, Zhou R, Verma AD, Xia B. CD4(+)T cells: differentiation and functions. Clin Dev Immunol. 2012;2012:925135.

23.   Mahnke YD, Beddall MH, Roederer M. OMIP-017: human CD4(+) helper T-cell subsets including follicular helper cells. Cytometry A. 2013;83(5):439-40.

24.   Karnell JL, Dimasi N, Karnell FG, 3rd, Fleming R, Kuta E, Wilson M, et al. CD19 and CD32b differentially regulate human B cell responsiveness. J Immunol. 2014;192(4):1480-90.

25.   Lucas CR, Cordero-Nieves HM, Erbe RS, McAlees JW, Bhatia S, Hodes RJ, et al. Prohibitins and the cytoplasmic domain of CD86 cooperate to mediate CD86 signaling in B lymphocytes. J Immunol. 2013;190(2):723-36.

26.   Sucur A, Jajic Z, Artukovic M, Matijasevic MI, Anic B, Flegar D, et al. Chemokine signals are crucial for enhanced homing and differentiation of circulating osteoclast progenitor cells. Arthritis Res Ther. 2017;19(1):142.

27.   Radulovic K, Niess JH. CD69 is the crucial regulator of intestinal inflammation: a new target molecule for IBD treatment? J Immunol Res. 2015;2015:497056.

28.   Bruggner RV, Bodenmiller B, Dill DL, Tibshirani RJ, Nolan GP. Automated identification of stratifying signatures in cellular subpopulations. Proc Natl Acad Sci U S A. 2014;111(26):E2770-7.

29.   O'Neill SK, Cao Y, Hamel KM, Doodes PD, Hutas G, Finnegan A. Expression of CD80/86 on B cells is essential for autoreactive T cell activation and the development of arthritis. J Immunol. 2007;179(8):5109-16.

30.   Smith KG, Clatworthy MR. FcgammaRIIB in autoimmunity and infection: evolutionary and therapeutic implications. Nat Rev Immunol. 2010;10(5):328-43.

31.   Robinson WH, Mao R. Biomarkers to guide clinical therapeutics in rheumatology? Curr Opin Rheumatol. 2016;28(2):168-75.

32.   Kimball AK, Oko LM, Bullock BL, Nemenoff RA, van Dyk LF, Clambey ET. A Beginner's Guide to Analyzing and Visualizing Mass Cytometry Data. J Immunol. 2018;200(1):3-22.

33.   Mair F, Hartmann FJ, Mrdjen D, Tosevski V, Krieg C, Becher B. The end of gating? An introduction to automated analysis of high dimensional cytometry data. Eur J Immunol. 2016;46(1):34-43.

34.   James EA, Rieck M, Pieper J, Gebe JA, Yue BB, Tatum M, et al. Citrulline-specific Th1 cells are increased in rheumatoid arthritis and their frequency is influenced by disease duration and therapy. Arthritis Rheumatol. 2014;66(7):1712-22.

35.   Ciccia F, Guggino G, Ferrante A, Cipriani P, Giacomelli R, Triolo G. Interleukin-9 and T helper type 9 cells in rheumatic diseases. Clin Exp Immunol. 2016;185(2):125-32.

36.   Carvalheiro H, da Silva JA, Souto-Carneiro MM. Potential roles for CD8(+) T cells in rheumatoid arthritis. Autoimmun Rev. 2013;12(3):401-9.

37.   Carvalheiro H, Duarte C, Silva-Cardoso S, da Silva JA, Souto-Carneiro MM. CD8+ T cell profiles in patients with rheumatoid arthritis and their relationship to disease activity. Arthritis Rheumatol. 2015;67(2):363-71.

38.   Kondo T, Takiguchi M. Human memory CCR4+CD8+ T cell subset has the ability to produce multiple cytokines. Int Immunol. 2009;21(5):523-32.

39.   Marcinska K, Majewska-Szczepanik M, Lazar A, Kowalczyk P, Biala D, Wozniak D, et al. Epicutaneous (EC) immunization with type II collagen (COLL II) induces CD4(+) CD8(+) T suppressor cells that protect from collagen-induced arthritis (CIA). Pharmacol Rep. 2016;68(2):483-9.

40.   Quandt D, Rothe K, Scholz R, Baerwald CW, Wagner U. Peripheral CD4CD8 double positive T cells with a distinct helper cytokine profile are increased in rheumatoid arthritis. PLoS One. 2014;9(3):e93293.

41.   Sherlock JP, Joyce-Shaikh B, Turner SP, Chao CC, Sathe M, Grein J, et al. IL-23 induces spondyloarthropathy by acting on ROR-gammat+ CD3+CD4-CD8- entheseal resident T cells. Nat Med. 2012;18(7):1069-76.

42.   Brandt D, Hedrich CM. TCRalphabeta(+)CD3(+)CD4(-)CD8(-) (double negative) T cells in autoimmunity. Autoimmun Rev. 2018;17(4):422-30.

43.   Zahran AM, Saad K, Elsayh KI, Alblihed MA. Characterization of circulating CD4(+) CD8(+) double positive and CD4(-) CD8(-) double negative T-lymphocyte in children with beta-thalassemia major. Int J Hematol. 2017;105(3):265-71.

44.   D'Acquisto F, Crompton T. CD3+CD4-CD8- (double negative) T cells: saviours or villains of the immune response? Biochem Pharmacol. 2011;82(4):333-40.

45.   Firestein GS, McInnes IB. Immunopathogenesis of Rheumatoid Arthritis. Immunity. 2017;46(2):183-96.

46.   Bulati M, Buffa S, Martorana A, Gervasi F, Camarda C, Azzarello DM, et al. Double negative (IgG+IgD-CD27-) B cells are increased in a cohort of moderate-severe Alzheimer's disease patients and show a pro-inflammatory trafficking receptor phenotype. J Alzheimers Dis. 2015;44(4):1241-51.

47.   Nagafuchi Y, Shoda H, Sumitomo S, Nakachi S, Kato R, Tsuchida Y, et al. Enhanced gut homing receptor expression of unswitched memory B cells in rheumatoid arthritis. Clin Exp Rheumatol. 2017;35(2):354-5.

48.   Mauri C, Jury EC. Could the expression of CD86 and FcgammaRIIB on B cells be functionally related and involved in driving rheumatoid arthritis? Arthritis Res Ther. 2010;12(4):133.

49.   Magnusson SE, Engstrom M, Jacob U, Ulfgren AK, Kleinau S. High synovial expression of the inhibitory FcgammaRIIb in rheumatoid arthritis. Arthritis Res Ther. 2007;9(3):R51.

50.   Catalan D, Aravena O, Sabugo F, Wurmann P, Soto L, Kalergis AM, et al. B cells from rheumatoid arthritis patients show important alterations in the expression of CD86 and FcgammaRIIb, which are modulated by anti-tumor necrosis factor therapy. Arthritis Res Ther. 2010;12(2):R68.

51.   Dominguez-Pantoja M, Lopez-Herrera G, Romero-Ramirez H, Santos-Argumedo L, Chavez-Rueda AK, Hernandez-Cueto A, et al. CD38 protein deficiency induces autoimmune characteristics and its activation enhances IL-10 production by regulatory B cells. Scand J Immunol. 2018;87(6):e12664.

52.   Cole S, Walsh A, Yin X, Wechalekar MD, Smith MD, Proudman SM, et al. Integrative analysis reveals CD38 as a therapeutic target for plasma cell-rich pre-disease and established rheumatoid arthritis and systemic lupus erythematosus. Arthritis Res Ther. 2018;20(1):85.

53.   He C, Li D, Gao J, Li J, Liu Z, Xu W. Inhibition of CXCR4 inhibits the proliferation and osteogenic potential of fibroblasts from ankylosing spondylitis via the Wnt/betacatenin pathway. Mol Med Rep. 2019;19(4):3237-46.

54.   Aeberli D, Kamgang R, Balani D, Hofstetter W, Villiger PM, Seitz M. Regulation of peripheral classical and non-classical monocytes on infliximab treatment in patients with rheumatoid arthritis and ankylosing spondylitis. RMD Open. 2016;2(1):e000079.

55.   Zgraggen S, Huggenberger R, Kerl K, Detmar M. An important role of the SDF-1/CXCR4 axis in chronic skin inflammation. PLoS One. 2014;9(4):e93665.

56.   Lebre MC, Vergunst CE, Choi IY, Aarrass S, Oliveira AS, Wyant T, et al. Why CCR2 and CCR5 blockade failed and why CCR1 blockade might still be effective in the treatment of rheumatoid arthritis. PLoS One. 2011;6(7):e21772.

57.   Ikic M, Jajic Z, Lazic E, Ivcevic S, Grubisic F, Marusic A, et al. Association of systemic and intra-articular osteoclastogenic potential, pro-inflammatory mediators and disease activity with the form of inflammatory arthritis. Int Orthop. 2014;38(1):183-92.

Table 1. Demographic and clinical characteristics of enrolled patients with rheumatoid arthritis, ankylosing spondylitis and psoriatic arthritis

	Ankylosing spondylitis	Rheumatoid arthritis	Psoriatic arthritis	Controls
Age (years)	60 [52-66]	66 [52-73]	55 [51-64]	55 [43-68]
Gender (male/female)	9/13	3/27	9/13	6/18
Disease duration (years)	22 [14-29]	15 [7-21]	15 [10-21]	
BASDAI	6.07 [4.90-7.21]	-	7.31 [5.71-8.30]	
ASDAS	2.91 [2.41-3.46]	-	3.51 [2.94-4.12]	
DAS28	4.73 [3.1-6.1]	6.2 [5.1-6.5]	5.6 [4.6-6.3]	
DAPSA	-	-	46.5 [36.5-54.6]	
CDAI	30.6 [20.0-66.6]	40.9 [24.8-44.2]	35.4 [17.5-45.1]	
ESR (mm/h)	10 [4.0-16.0]	24.0 [18.0-31.0]	15.0 [8.5-29.0]	
CRP (mg/L)	3.7 [0.65-15.6]	9.4 [3.1-19.6]	7.5 [2.5-12.7]	
RF (IU/L)	-	38.6 [10.7-75.9]	-	
aCPA (EU/L)	-	3.7 [1.1-284.5]	-	
Tender joint count (28; 66/68)	26 [10-45]	17 [12-22]	15 [6-26]	
Swollen joint count (28 score)	1 [0-2]	7 [1-15]	5 [1-12]	
Disease activity (physician VAS)	7.3 [5.9-8.6]	6.7 [4.8-8.7]	6.5 [6.0-7.0]	
Disease activity (patient VAS)	7.0 [6.0-8.5]	7.2 [5.7-8.9]	6.7 [6.2-7.7]	
Disease activity (high/moderate)	18/4	22/8	12/10	

*Values are presented as median with interquartile range. ASDAS – Ankylosing Spondylitis Disease Activity Score; BASDAI – Bath Ankylosing Spondylitis Disease Activity Index; ESR – erythrocyte sedimentation rate; CRP – C-reactive protein, CDAI – clinical disease activity

index; DAS28 – disease activity score including a 28-joint count (calculated with ESR); DAPSA – Disease Activity index for PSoriatic Arthritis; VAS – visual analog scale (cm); RF – rheumatoid factor (determined by turbidimetry), aCPA - anti-citrullinated protein antibodies (determined by ELISA), Tender joint count – 28 for RA and PsA, 66/68 for AS. Therapy consisted of non-steroid anti-inflammatory drugs (NSAID) for AS (mostly ibuprofen 600 mg twice a day), a combination of NSAID and disease-modidying anti-rheumatic drugs (DMARD) for PsA (mostly ibuprofen 600 mg twice a day and methotrexate 15 mg once a week), and a combination of NSAID, DMARD and/or glucocorticoid for RA (mostly ibuprofen 600 mg twice a day and methotrexate 15 mg once a week or methylprednisolone 4 mg once a day). Moderate disease activity was defined as $3.2 < DAS28 \leq 5.1$ in RA, $2.1 < ASDAS \leq 3.5$ in AS, and $14 < DAPSA \leq 28$ in PsA. High disease activity was defined as $DAS28 > 5.1$ in RA, $ASDAS > 3.5$ in AS, and $DAPSA > 28$ in PsA. There were no remitting or low disease activity patients included in the study.

Table 2. Phenotype of analyzed circulating immune cell subpopulations

Subpopulation	Phenotype
helper T-cells	
Th1-like	$CD3^+CD4^+CCR4\text{-}CCR6\text{-}$
Th2	$CD3^+CD4^+CCR4^+CCR6\text{-}$
Th9	$CD3^+CD4^+CCR4^-CCR6^+$
Th17	$CD3^+CD4^+CCR4^+CCR6^+$
cytotoxic T-cells	
immature effector memory	$CD3^+CD8^+CCR4^+$
early effector memory	$CD3^+CD8^+CCR6^+$
follicular	$CD4^+CD8^+CXCR5^+$
B-cells	
naïve	$CD19^+IgD^+CD27^-$
unswitched memory	$CD19^+IgD^+CD27^+$
class-switched memory	$CD19^+IgD^-CD27^+$
double-negative memory	$CD19^+IgD^-CD27^-$
plasmablasts	$CD19^+IgD^-CD27^+CD38^+$
monocytes	
mature (classical) monocytes	$CD3^-CD19^-CD56CD11b^+CD14^+$
osteoclastogenic monocytes	$CD3^-CD19^-CD56^-CD11b^+CD14^+CD115^+$

Supplementary table 1. Antibody-producing clones for the analyzed immune cell markers

Marker	Antibody-producing clone
CD3	OKT3
CD4	RPA-T4
CD8	RPA-T8
CD19	HIB19
CD27	O323
CD32B	FAB1330G
CD38	HIT2
CD86	BU63
CCR1	FAB145G
CCR2	FAB151P
CCR4	FAB1567P
CCR6	FAB590G
CXCR4	FAB170G
CXCR5	FAB190G
IgD	IA6-2

Supplementary table 2. Comparison of T-cell subpopulations in peripheral blood and synovial fluid from rheumatoid arthritis and psoriatic arthritis patients

Population	Diagnosis	Blood (%)	Synovial fluid (%)	p
double-positive T cells	RA	0.52 [0.4-0.9]	0.97 [0.6-2.2]	0.204
	PsA	1.0 [0.4-4.1]	1.72 [0.9-1.74]	0.611
double-negative T cells	RA	4.9 [3.1-6.5]	13.8 [6.1-20.2]	0.034
	PsA	2.3 [2.1-3.6]	2.9 [2.4-4.5]	0.363
Th1-like cells	RA	80.9 [77.6-86.5]	75.1 [67.0-81.8]	0.050
	PsA	77.8 [75.9-84.4]	76.1 [63.6-78.9]	0.295
$CXCR5^+$ cytotoxic T cells	RA	13.6 [10.5-15.6]	3.7[1.7-10.6]	0.004
	PsA	1.3 [1.0-2.4]	2.2 [1.5-3.4]	0.296
$CCR6^+$ cytotoxic T cells	**RA**	**2.8 [1.1-4.2]**	**5.2 [3.9-6.8]**	**0.017**
	PsA	0.6 [0.4-1.1]	3.1 [2.5-3.9]	0.004

*Values are presented as median with interquartile range. Only subpopulations significantly changed in blood of at least one disease were compared and shown. Subpopulations which were significantly increased in synovial fluid in addition to the original finding in blood are bolded. Blood-to-synovial fluid comparison was performed using Mann-Whitney test. Synovial fluid for RA n=8, PsA n=3. PsA – psoriatic arthritis; RA – rheumatoid arthritis.

Supplementary table 3. Comparison of B-cell subpopulations in peripheral blood and synovial fluid from rheumatoid arthritis and psoriatic arthritis patients

Population	Diagnosis	Blood (%)	Synovial fluid (%)	p
naïve B-cells	RA	60.0 [55.1-73.4]	22.1 [17.6-31.6]	<0.001
	PsA	**67.8 [58.6-71.5]**	**13.5 [8.3-18.8]**	**0.019**
CD32B$^+$ naïve B-cells	**RA**	**1.1 [0.5-2.6]**	**91.7 [81.4-96.3]**	**<0.001**
	PsA	**2.0 [0.9-2.9]**	**67.1 [57.5-76.6]**	**0.017**
CD32B$^+$ memory B-cells	**RA**	**4.4 [2.1-7.4]**	**71.8 [35.9-86.1]**	**<0.002**
	PsA	**7.2 [3.3-11.2]**	**60.0 [44.0-75.9]**	**0.017**

*Values are presented as median with interquartile range. Only subpopulations significantly changed in blood of at least one disease were compared and shown. Subpopulations which were significantly increased in synovial fluid in addition to the original finding in blood are bolded. Blood-to-synovial fluid comparison was performed using Mann-Whitney test. Synovial fluid for RA n=8, PsA n=3. PsA – psoriatic arthritis; RA – rheumatoid arthritis.

Figure legends

Figure 1. T-cell subpopulations in peripheral blood of arthritic patients. **(A)** Frequencies of helper (CD4$^+$CD8$^-$), cytotoxic (CD4$^-$CD8$^+$), double-positive (CD4$^+$CD8$^+$) and double negative (CD4$^-$CD8$^-$) T-cells of control (CTRL) subjects and rheumatoid arthritis (RA), ankylosing spondylitis (AS) and psoriatic arthritis (PsA). **(B)** Frequencies of Th1-like (CCR4$^-$CCR6$^-$), Th2 (CCR4$^+$CCR6$^-$), Th9 (CCR4$^-$CCR6$^+$), Th17 (CCR4$^+$CCR6$^+$) and Tfh (CXCR5$^+$) cells. **(C)** Frequencies of immature effector memory (CCR4$^+$), early effector memory (CCR6$^+$) and follicular (CXCR5$^+$) cytotoxic T-cell subpopulations. Values are presented as medians (square), with boundaries (horizontal lines) representing interquartile range (IQR), and circles representing individual samples values. Disease-to-control comparisons were performed using non-parametric Mann-Whitney test, p values <0.05 are shown.

Figure 2. Correlation of clinical parameters and significantly changed lymphocyte subpopulations in peripheral blood of rheumatoid arthritis, psoriatic arthritis and ankylosing spondylitis. Association was established using rank correlation. Correlations were calculated only for significantly changed cell populations, of which those with p<0.05 and Spearman´s coefficient ρ>0.5 or ρ<-0.5 are shown. Significant strongly positive (ρ>0.5 and p<0.05) correlations are marked with green, significant strongly negative (ρ<-0.5 and p<0.05) correlations are marked with red, variable self-correlation is marked yellow and unsignificant correlations are unmarked. ASDAS - Ankylosing Spondylitis Disease Activity Score; BASDAI - Bath Ankylosing Spondylitis Disease Activity Index; ESR – erythrocyte sedimentation rate; CDAI – clinical disease activity index; DAS28 – Disease Activity Score out of 28 joint count; SJC – swollen joint count (out of 28); TJC – tender joint count (out of 28); AS – ankylosing spondylitis; PsA – psoriatic arthritis; RA – rheumatoid arthritis.

Figure 3. B-cell subpopulations in peripheral blood of arthritic patients. **(A)** Frequencies of naïve (IgD$^+$CD27$^-$), class-unswitched memory (IgD$^+$CD27$^+$), class-switched memory (IgD$^-$CD27$^+$), double-negative memory (IgD$^-$CD27$^-$) and plasmablast (IgD$^-$CD27$^+$CD38^{hi}) B-cells of control (CTRL) subjects and rheumatoid arthritis (RA), ankylosing spondylitis (AS) and psoriatic arthritis (PsA). **(B)** Expression of inhibitory Fc-receptor CD32B on B-cell subpopulations. Values are presented as medians (square), with boundaries (horizontal lines) representing interquartile range (IQR), and circles representing individual samples values. Disease-to-control comparisons were performed using non-parametric Mann-Whitney test, p values <0.05 are shown.

Figure 4. Citrus automated flow cytometry analysis and disease associated subset selection for T-cell panel in arthritic patients. **(A)** Visual representation of unsupervised hierarchical clustering by Citrus. The analysis was done on CD3$^+$ cells, while CD4, CD8, CCR4, CCR6 and CXCR5 were used as markers for clustering. The color scale indicates median intensity of respective marker expression, while node size is relative to the frequency of cells in the cluster. Red circle indicates the source cluster at the start of automated hierarchical gating which includes all cells, while red arrows indicate significantly different clusters. **(B)** Histograms of marker expression and relative abundance of disease-associated cell clusters. Analysis of clusters was done on account of abundance in the cluster between groups using "significance analysis of microarrays" (sam) model. Histograms show the marker expression profile for the cluster (red) versus background (purple) expression in all clusters. Results are mean fold change ± SEM. Disease-to-control comparisons were performed using non-parametric Mann-Whitney test, clusters for p values <0.05 are shown.

Figure 5. Citrus automated flow cytometry analysis and disease associated subset selection for B-cell panel in arthritic patients. **(A)** Visual representation of unsupervised hierarchical clustering by Citrus. The analysis was done on $CD19^+$ cells, while IgD, CD27, CD32B, CD38 and CD86 were used as markers for clustering. The color scale indicates median intensity of respective marker expression, while node size is relative to the frequency of cells in the cluster. Red circle indicates the source cluster at the start of automated hierarchical gating which includes all cells, while red arrows indicate significantly different clusters. **(B)** Histograms of marker expression and relative abundance of disease-associated cell clusters. Analysis of clusters was done on account of abundance in the cluster between groups using "significance analysis of microarrays" (sam) model. Histograms show the marker expression profile for the cluster (red) versus background (purple) expression in all clusters. Results are mean fold change ± SEM. Disease-to-control comparisons were performed using non-parametric Mann-Whitney test, clusters for p values <0.05 are shown.

Figure 6. In vitro lymphocyte proliferation and activation assay. **(A)** CD69 (activation marker) relative expression on T-cells and B-cells of control (CTRL), rheumatoid arthritis (RA), ankylosing spondylitis (AS) and psoriatic arthritis (PsA) samples in comparison to untreated control. **(B)** Percentage of divided T-cells and B-cells from peripheral blood of CTRL, RA, AS and PsA samples. Values are presented as medians (middle line), with boxes representing interquartile range (IQR), whiskers representing 1.5 times the IQR and squares or circles representing outliers. Disease-to-control comparisons were performed using non-parametric Mann-Whitney test, p values <0.05 are shown.

Figure 7. Expression of chemokine receptors on peripheral osteoclast progenitor-enriched monocytes in arthritic patients. Expression of CCR1, CCR2, CCR4 and CXCR4 on CD3$^-$CD19$^-$CD56$^-$CD11b$^+$CD14$^+$CD115$^+$ monocytes of control (CTRL), rheumatoid arthritis (RA), ankylosing spondylitis (AS) and psoriatic arthritis (PsA) patients. Values are presented as medians (square), with boundaries (horizontal lines) representing interquartile range (IQR), and circles representing individual samples values. Disease-to-control comparisons were performed using non-parametric Mann-Whitney test, p values <0.05 are shown.

Figure 8. Citrus automated flow cytometry analysis and disease associated subset selection for monocyte panels in arthritic patients. Visual representation of unsupervised hierarchical clustering by Citrus and histograms of marker expression and relative abundance of disease-associated cell clusters. **(A)** Analysis done on CD3$^-$CD19$^-$CD56$^-$CD11b$^+$ cells, with CD14, CD115, CCR1 and CXCR4 as markers for clustering. **(B)** Analysis done on CD3$^-$CD19$^-$CD56$^-$CD11b$^+$ cells, with CD14, CD115, CCR2 and CCR4 as markers for clustering. The color scale indicates median intensity of respective marker expression, while node size is relative to the frequency of cells in the cluster. Red circle indicates the source cluster at the start of automated hierarchical gating which includes all cells, while red arrows indicate significantly different clusters. Histograms of marker expression and relative abundance of disease-associated cell clusters. Analysis of clusters was done on account of abundance in the cluster between groups using "significance analysis of microarrays" (sam) model. Histograms show the marker expression profile for the cluster (red) versus background (purple) expression in all clusters. Results are mean fold change ± SEM. Disease-to-control comparisons were performed using non-parametric Mann-Whitney test, clusters for p values <0.05 are shown.

Figure 9. Disease-specific immune subpopulations in rheumatoid arthritis, ankylosing spondylitis and psoriatic arthritis. The diagram summarises pathognomonic circulating immune cell subpopulations in three rheumatic diseases. Our results suggest significant phenotypic and functional abnormalities in B-cell subsets in ankylosing spondylitis, cytotoxic T-cell subsets in rheumatoid arthritis, and chemokine receptor expressing monocyte subsets in all three diseases. Changes in immune subsets were less polarized in PsA patients. AS – ankylosing spondylitis; PsA – psoriatic arthritis; RA – rheumatoid arthritis.

Supplementary figure 1. Flow cytometry gating strategy and frequency of general peripheral lymphocyte and monocyte subpopulations in arthritic patients. **(A)** Gating strategy for T-cells. $CD3^+$ T-cells were dissected into $CD4^+$ helper T-cell (Th), $CD8^+$ cytotoxic T-cells (Tc), $CD4^+CD8^+$ double-positive T-cells (DP) or $CD4^-CD8^-$ double-negative T-cells (DN). Helper T-cell populations were segregated into Th1-like, Th2, Th9, Th17 and Tfh. Cytotoxic T-cell populations were segregated into immature effector memory ($CCR4^+$), early effector memory ($CCR6^+$) and follicular ($CXCR5^+$) cytotoxic T-cell subpopulations. **(B)** Gating strategy for B-cells. $CD19^+$ B-cells were disected into naïve, class-switched (memCS), unswitched (memUS) and double-negative (memDN) memory B-cells; each population was further analyze for the expression of CD32B and CD86. **(C)** Gating strategy for monocytes. Lymphoid negative myeloid cells were dissected into myeloid ($CD11b^+$), monocyte ($CD14^+$) and osteoclastogenic monocyte ($CD115^+$) subsets, and further analysed for the expression of chemokine receptors CCR1, CCR2, CCR4, CXCR4. **(D)** Proportion of T-cells, B-cells and monocytes in peripheral blood of control (CTRL) subjects and rheumatoid arthritis (RA), ankylosing spondylitis (AS) and psoriatic arthritis (PsA) patients. Values are presented as medians (square), with boundaries (horizontal lines) representing interquartile range (IQR), and circles representing individual

values. Disease-to-control comparisons were performed using non-parametric Mann-Whitney test, p values <0.05 are shown.

Supplementary figure 2. Comparison of selected lymphocyte subpopulations in peripheral blood mononuclear cells and disease activity indices before, one and three months after start of anti-TNF therapy in rheumatoid arthritis, psoriatic arthritis and ankylosing spondylitis patients. Results are presented as individual values and medians (square) with connecting lines. Only selected subpopulations previously detected as significantly changed in blood are shown. DAS28 values are shown for RA and PsA patients, ASDAS and BASDAI for AS and PsA, while DAPSA only for PsA. AS – ankylosing spondylitis; PsA – psoriatic arthritis; RA – rheumatoid arthritis; ASDAS – Ankylosing spondylitis disease activity score; BASDAI – Bath ankylosing spondylitis disease activity index; DAS28 – Disease activity score including a 28-joint count (calculated with ESR); DAPSA – Disease activity index for psoriatic arthritis; * denotes significant difference for paired sample comparison of the respective disease. Comparisons were performed using Wilcoxon signed-rank test, p values <0.05 were considered significant.

Supplementary figure 3. Treatment of osteoclastogenic culture by lymphocyte-conditioned supernatants. Peripheral osteoclast progenitors (OCPs) were defined within monocyte fraction as $CD3^-CD19^-CD56^-CD11b^+CD14^+$ subset and sorted using BD FacsARIA II instrument. Sorted OCPs were plated at a density of 4×10^4 cells per well in 96-well plate in α-MEM/10% FBS and osteoclastogenic growth factors, 30 ng/mL macrophage colony-stimulating factor (M-CSF) and 100 ng/mL rh receptor activator of nuclear factor-kappaB ligand (RANKL). Conditioned media were added in dilution of 1:3 from unstimulated (Ø) or mitogenically (MIT)

stimulated control (CTRL) or rheumatoid arthritis (RA) supernatants. At day 11–13 of culture, osteoclast were determined as TRAP$^+$ cells with two or more nuclei per cell. Results are mean ± SD. Group-to-group comparisons were performed using ANOVA with Student-Newman-Keuls post-hoc test, p values <0.05 were considered significant. * denotes significant change versus unstimulated supernatant; ** denotes significant change versus stimulated control supernatant.

List of abbreviations

aCPA – anti-citrullinated protein antibodies

ANOVA – analysis of variance

APC – allophycocyanine

AS – ankylosing spondylitis

CCR – C-C chemokine receptor

CDAI – Clinical disease activity index

CRP – C-reactive protein

CTRL – control

CXCR – C-X-C chemokine receptor

DAS28 – Disease activity score including a 28-joint count

DMARD – disease-modifying antirheumatic drugs

DN – double negative

DP – double positive

ESR – erythrocyte sedimentation rate

FACS – fluorescence-activated cell sorting

FBS – fetal bovine serum

FITC – fluorescein isothiocyanate

IL – interleukin

IQR – interquartile range

M-CSF – macrophage colony-stimulating factor

NSAID – non-steroidal anti-inflammatory

OCP – osteoclast progenitor

PBMC – peripheral blood mononuclear cells

PBS – phosphate-buffered saline

PE – phycoerythrin

PE-Cy7 – phycoerythrin-cyanine7

PerCP - Cy5.5 – peridinin-chlorophyll-cyanine5.5

PsA – psoriatic arthritis

RA – rheumatoid arthritis

RANKL – receptor activator of nuclear factor-κB ligand

RF – rheumatoid factor

SJC – swollen joint count

TJC – tender joint count

TNF – tumor necrosis factor

TRAP – tartrate-resistant acid phosphatase

VAS – visual analogue scale

α-MEM – α-Minimal Essential Medium

Figure 1

A   T-cells
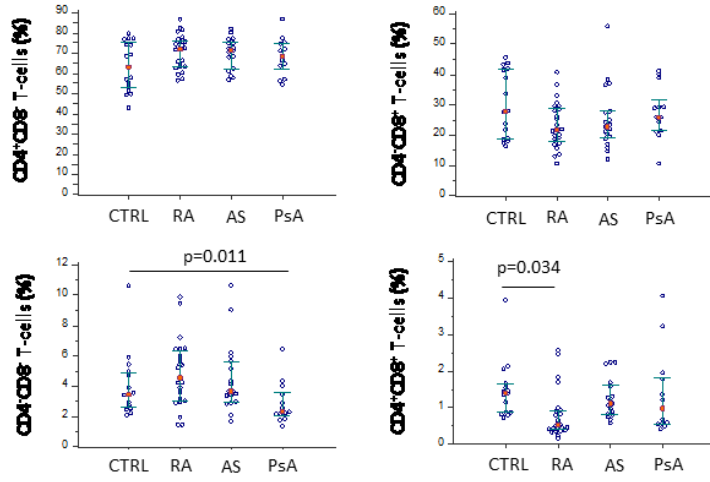
B   CD4+ T-cells
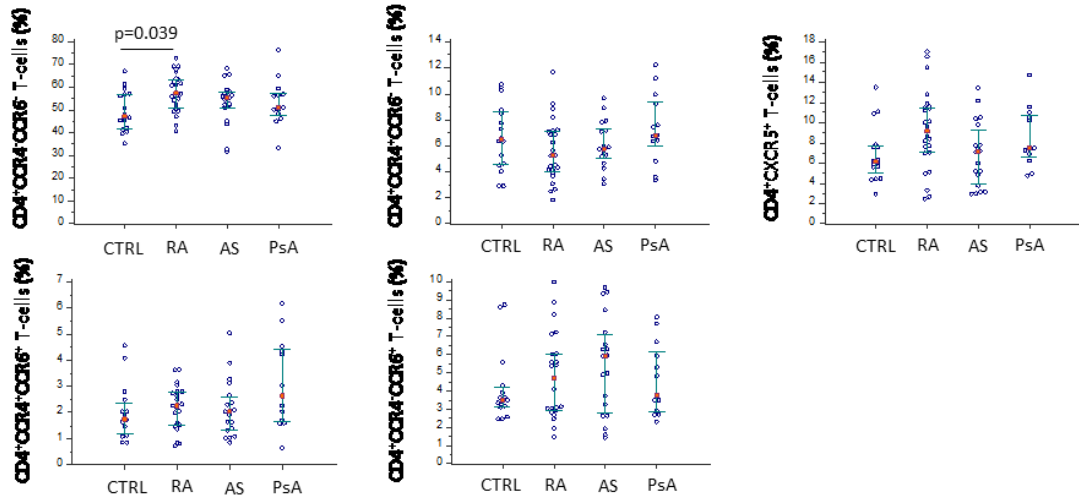
C   CD8+ T-cells
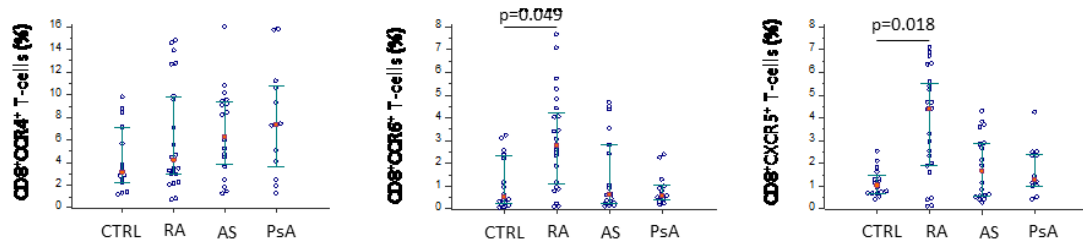
Figure 2
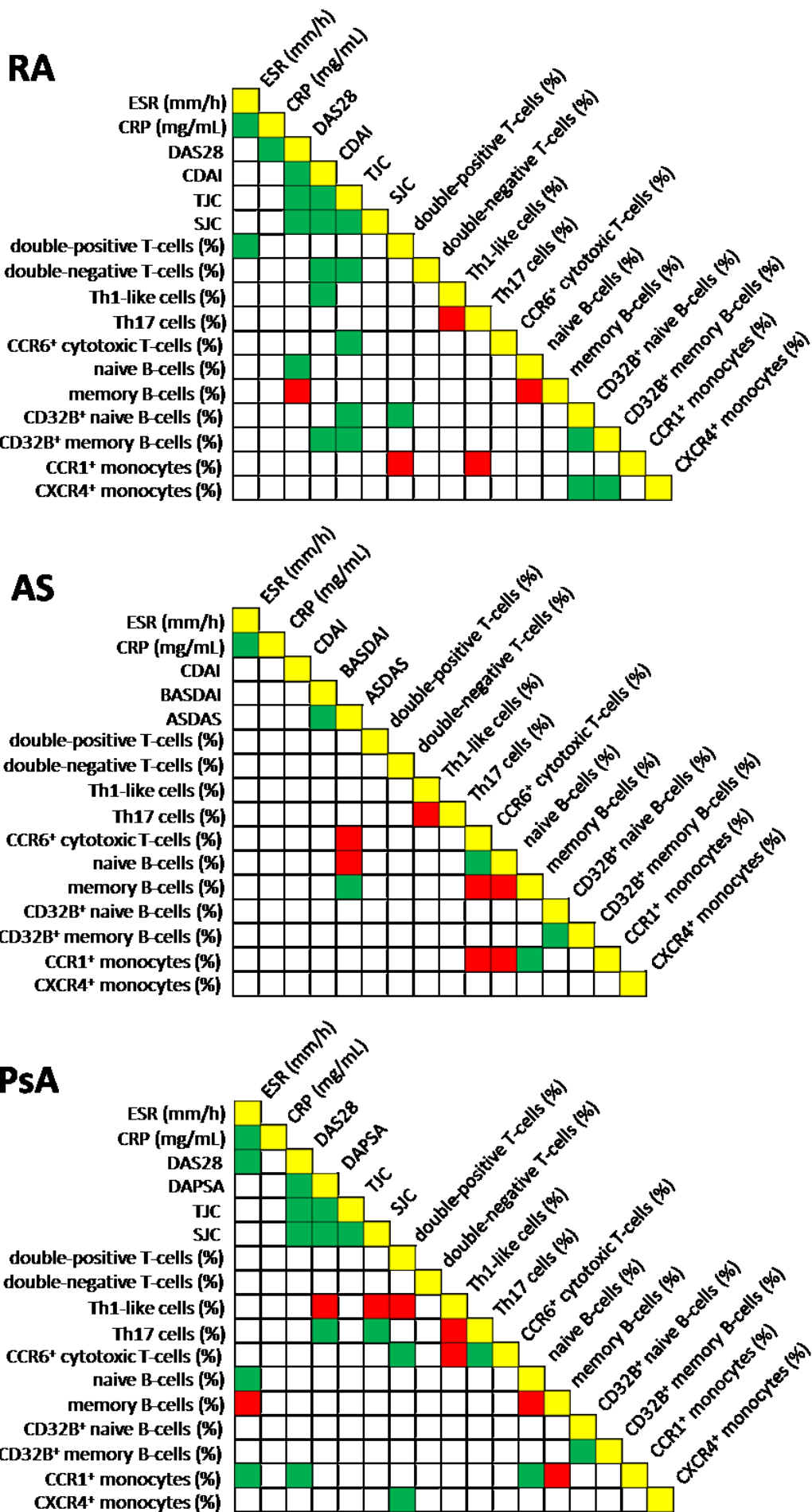
Figure 3

A   B-cells

B   CD32^{+} B-cells

Figure 4

A

CXCR5 · CD8 · CCR6 · CCR4 · CD4

B

CXCR5 · CD8 · CCR6 · CCR4 · CD4

cluster 279968 abundance

cluster 279969 abundance
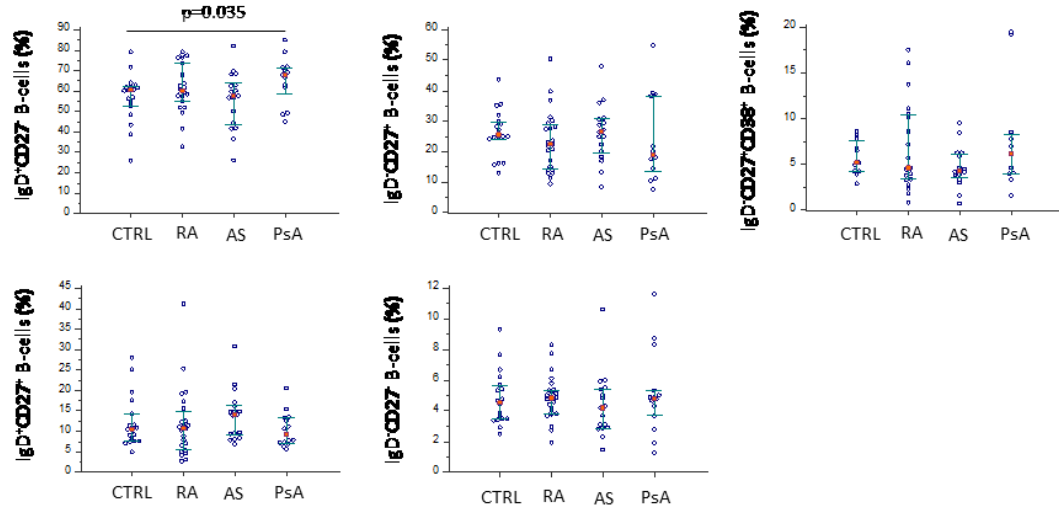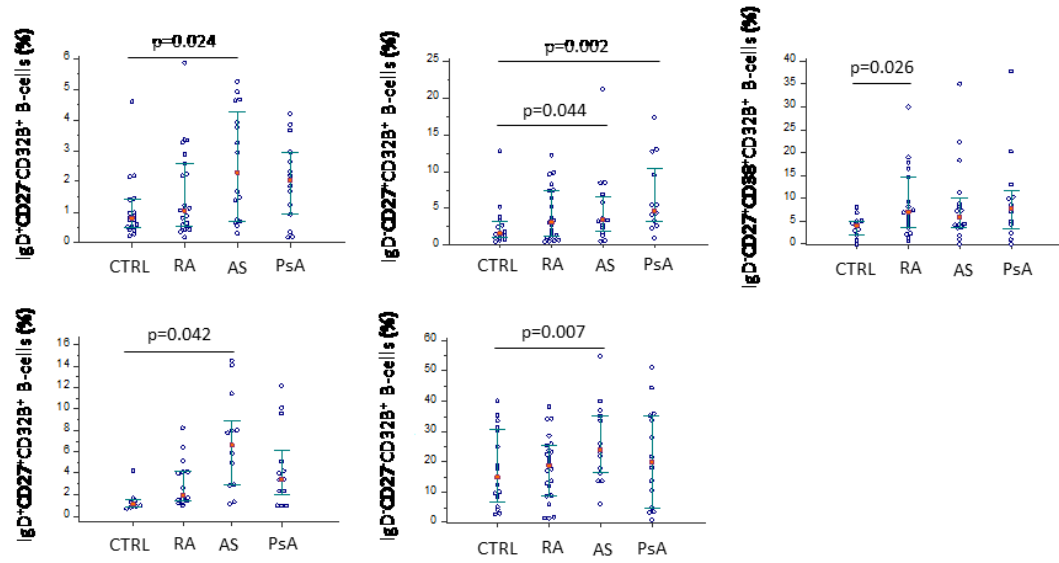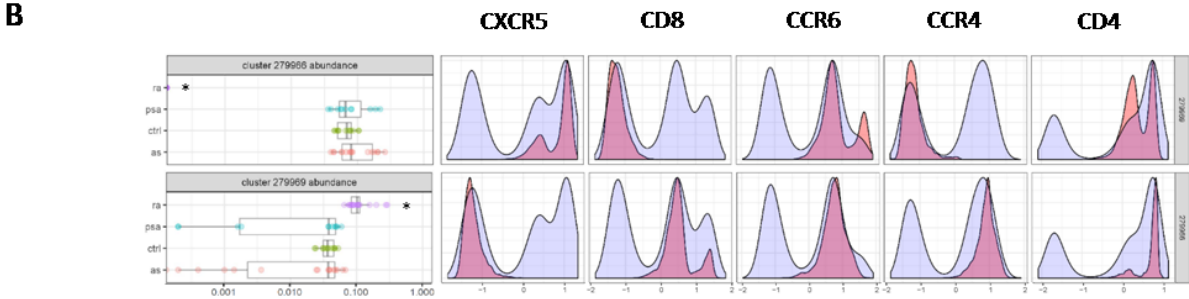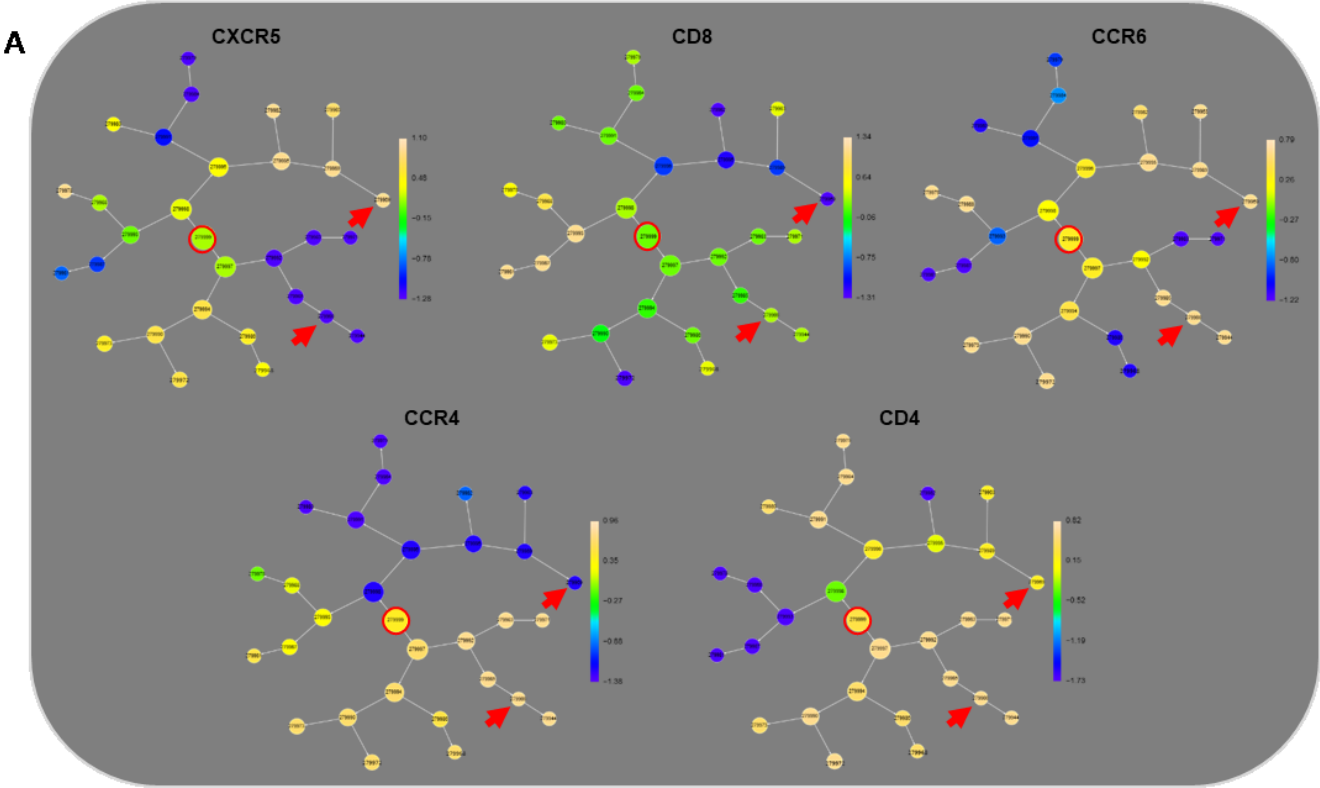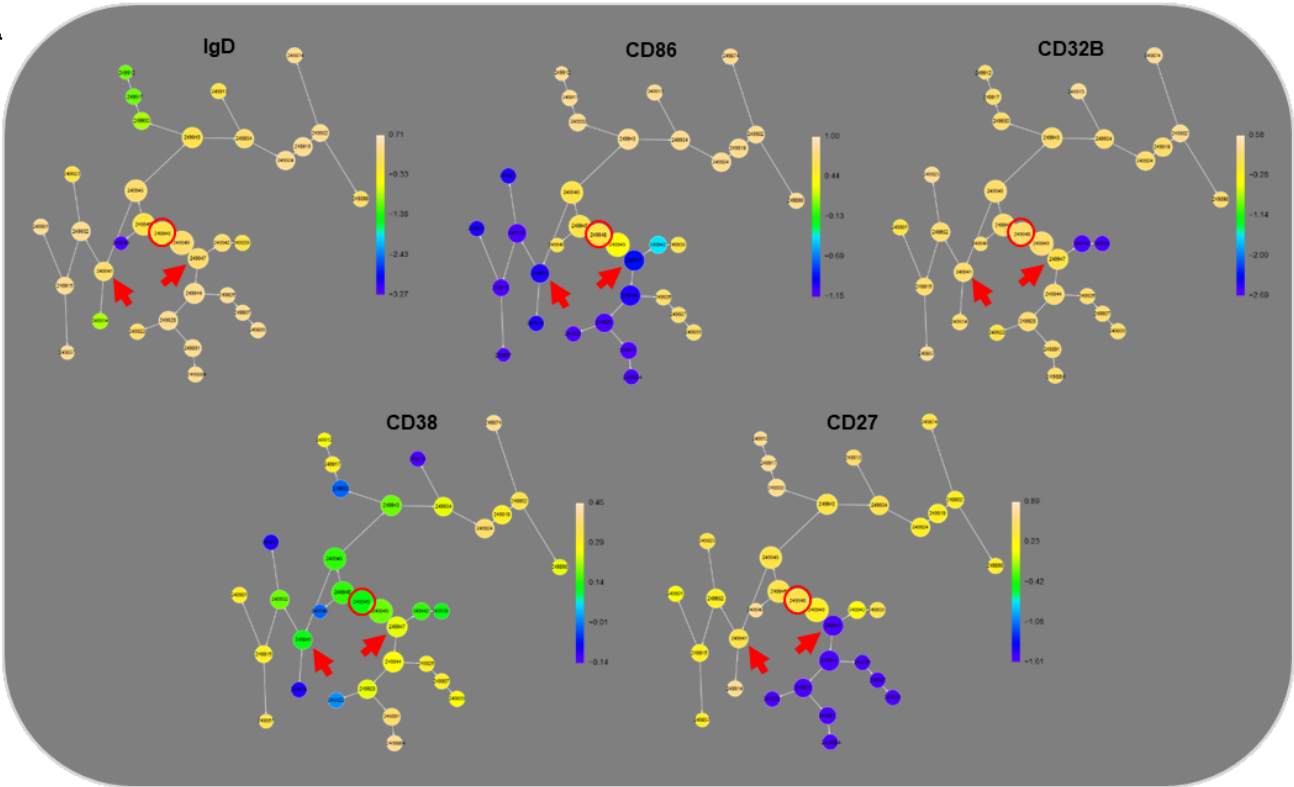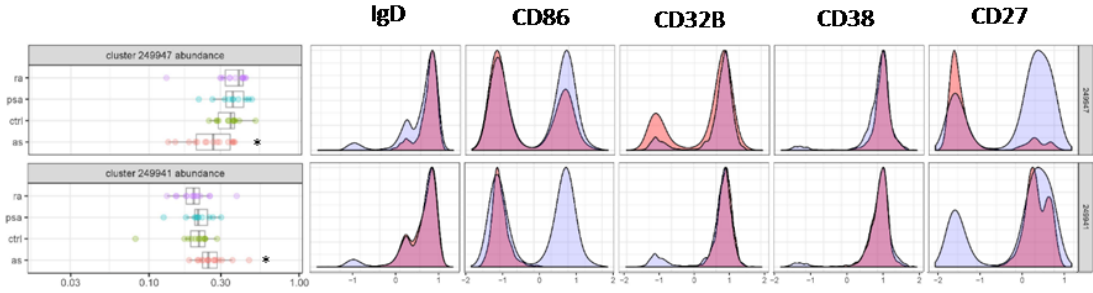
Figure 5

Figure 6
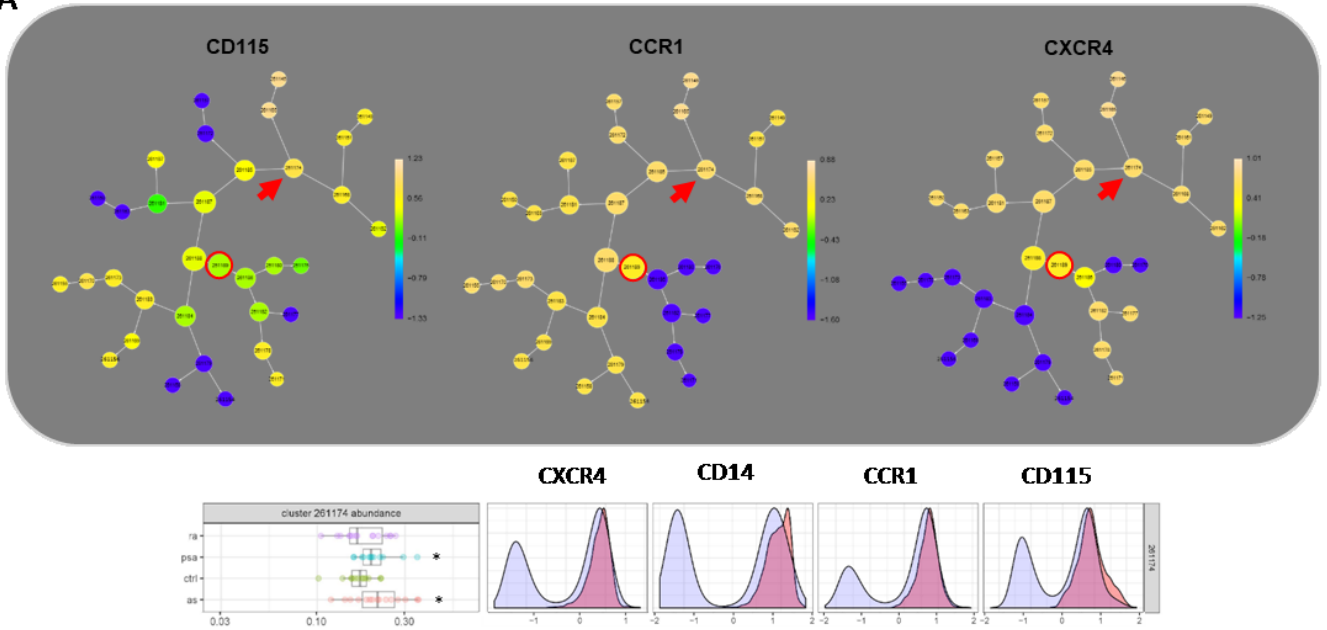
Figure 7

Figure 8

Figure 9

RA

AS

PsA

manual gating:
↓ double-positive T-cells
↑ CCR6⁺ cytotoxic T-cells
↑ CXCR5⁺ cytotoxic T-cells

Citrus:
↓ CCR4⁻CCR6⁺CXCR5⁺ helper T-cells
↑ CCR4⁺CCR6⁺CXCR5⁻ double-positive T-cells

manual gating:
↑ CD32B⁺ naive and memory B cells

Citrus:
↓ CD38⁺ naive B-cells
↑ CD32B⁺CD38⁺CD86⁻ unswitched B-cells
↑ CCR1⁺CXCR4⁺ monocytes
↓ CCR2⁻CCR4⁺ monocytes

manual gating:
↑ CCR1⁺ monocytes
↑ CXCR4⁺ monocytes
Citrus:
↑ CCR2⁺ monocytes

manual gating:
↓ double-negative T-cells
↓ CD86⁺ class-switched B-cells
Citrus:
↑ CCR1⁺CXCR4⁺ monocytes

Supplementary figure 1

A T-cell panel

B B-cell panel

C monocyte panel

D

Supplementary figure 2

Supplementary figure 3